

Supporting Information for ”Assimilation of both column- and layer-integrated dust opacity observations in the Martian atmosphere”

Tao Ruan¹, R. M. B. Young^{1,2}, S. R. Lewis³, L. Montabone^{1,4},

A. Valeanu¹ and P. L. Read¹

¹Atmospheric, Oceanic and Planetary Physics, Department of Physics, University of Oxford, Clarendon Laboratory, Parks Road,

Oxford, OX1 3PU, UK

²Department of Physics & National Space Science and Technology Center, UAE University, Al Ain, United Arab Emirates

³School of Physical Sciences, The Open University, Walton Hall, Milton Keynes, MK7 6AA, UK

⁴Space Science Institute, Boulder, CO 80301, USA

Contents of this file

1. S1. Additional figures for Verification against in-sample observations
2. S2. Additional figures for Reanalysis vs. MCD comparisons
3. Figures S1 to S15

Introduction In the following two sections we include additional figures that supplement the information provided in the main text. Section S1 presents additional figures showing the performance of the reanalyses against in-sample observations. Section S2 presents additional figures that provide in-depth comparisons between various climatological fields from the reanalysis and diagnostics obtained from the Mars Climate Database version 5.2.

S1. Verification against in-sample observations

The methods described in the main text were used to analyse various combinations of THEMIS and MCS observations obtained during Mars Years 28 and 29, representing a typical pair of years that include dusty seasons both with and without a planet encircling event. In this section we present results that evaluate the convergence of the assimilation towards the input data.

The model temperatures (either from the free-running model or the assimilated model state) were interpolated to the temperature retrieval pressure levels, before being converted to a global mean difference between model and observations. Figure S1 shows this difference averaged over several pseudo-height ranges (0–10 km, 10–20 km, 20–30 km, 30–40 km, and 40–80 km), assuming a 10 km scale height and a 610 Pa surface pressure. MCS retrievals are reported at pressure levels separated by around 1–1.5 km, while the true instrumental resolution is about 5 km (Kleinböhl et al., 2009), so this grouping of vertical levels smoothes the oversampled MCS retrievals over a distance larger than the true observational vertical resolution. Figure S2(a,b) shows the correlation between the assimilated THEMIS observations and the CIDO-only reanalysis and free-running model. Figure S3 shows the global-time mean difference in dust opacity between the in-sample observations and both the reanalysis and free-running model (see main text).

S2. Reanalysis vs. MCD comparisons Figures S6–S15 contain the complete set of comparisons made between the reanalysis and the Mars Climate Database. The following

quantities are included: surface temperature (Figs S4-S5), surface pressure (Figs S6-S7), atmospheric temperature (Figs S8-S9), density (Figs S10-S11), zonal velocity (Figs S12-S13), and meridional velocity (Figs S14-S15).

Surface quantities are monthly means (i.e. over 30 L_s) and atmospheric quantities are zonal-monthly means. Comparisons are made each month between MY28 $L_s = 120 - 150^\circ$ and MY29 $L_s = 330 - 360^\circ$ (20 months in total). Each plot shows the reanalysis monthly mean, MCD monthly mean, monthly mean difference (reanalysis minus MCD), reanalysis day-to-day variability, MCD day-to-day variability, and day-to-day variability ratio (reanalysis : MCD). The layout and format of each figure is the same.

References

- Kleinböhl, A., Schofield, J. T., Kass, D. M., Abdou, W. A., Backus, C. R., Sen, B., ...
McCleese, D. J. (2009). Mars Climate Sounder limb profile retrieval of atmospheric temperature, pressure, and dust and water ice opacity. *J. Geophys. Res.*, *114*(10), E10006. doi: 10.1029/2009JE003358

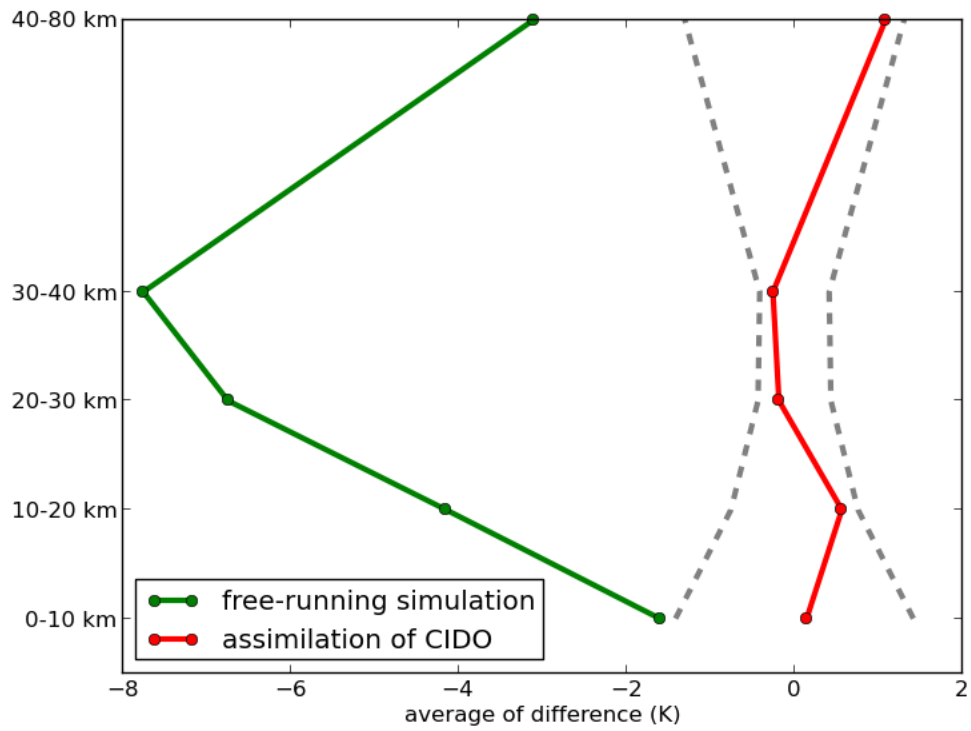


Figure S1. Global-time mean temperature difference between MCS observations and the free-running model (green) and CIDO-only reanalysis (red), during MY29 $L_s = 110^\circ - 330^\circ$. Grey dashed lines show the average uncertainty in the MCS observations (Kleinböhl et al., 2009).

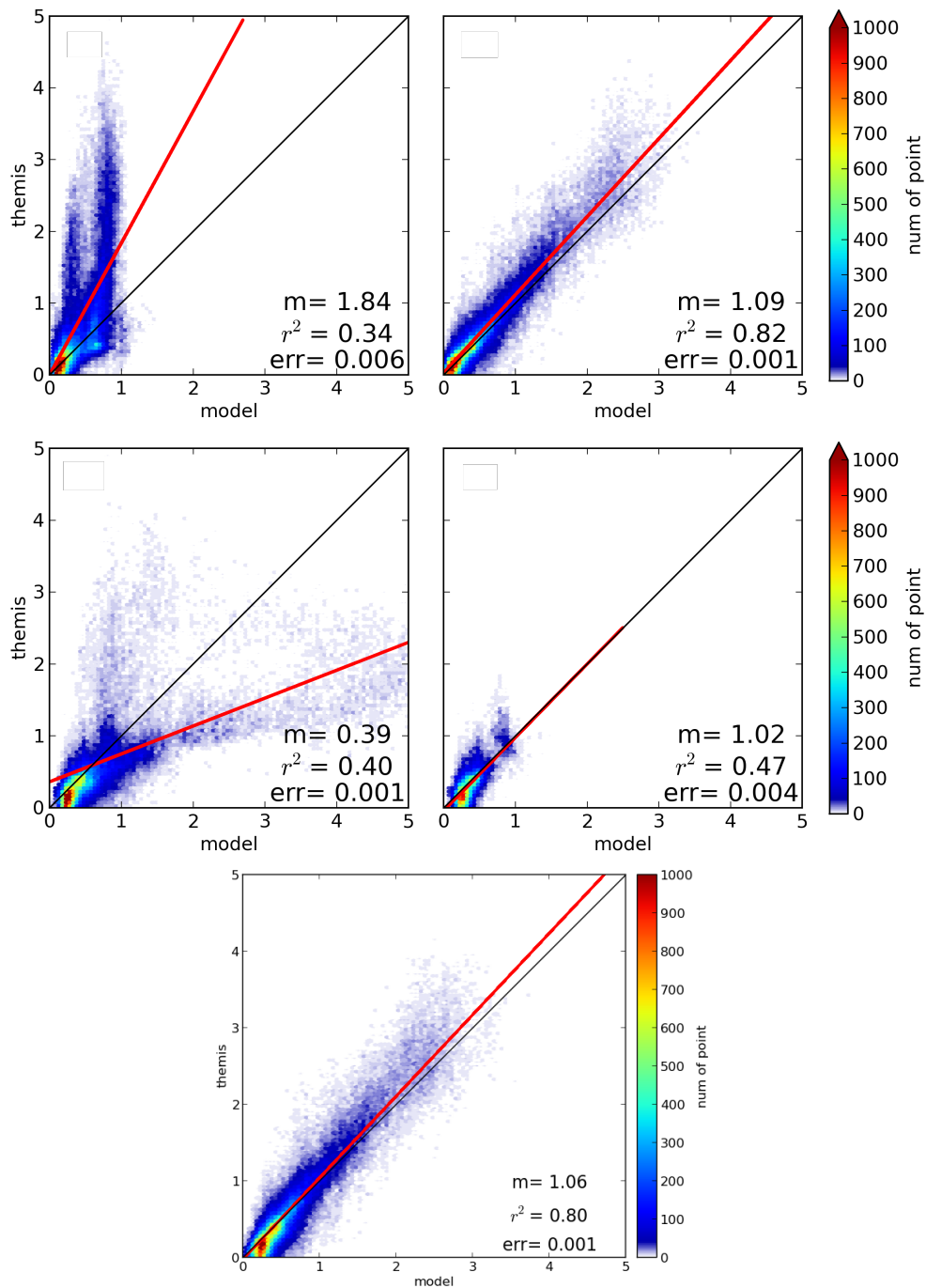


Figure S2. Scatter plots showing individual τ_{ref} points comparing the assimilated THEMIS observations with the free-running model and various reanalyses over the period shown in Fig. 4 of the main text. Colours show the data density as the number of points per square of side $\tau_{\text{ref}} = 0.05$. Red lines show the linear least square fit, with m the fitting coefficient, r^2 the coefficient of determination, and err the standard error in m . Black lines show $m = 1$.

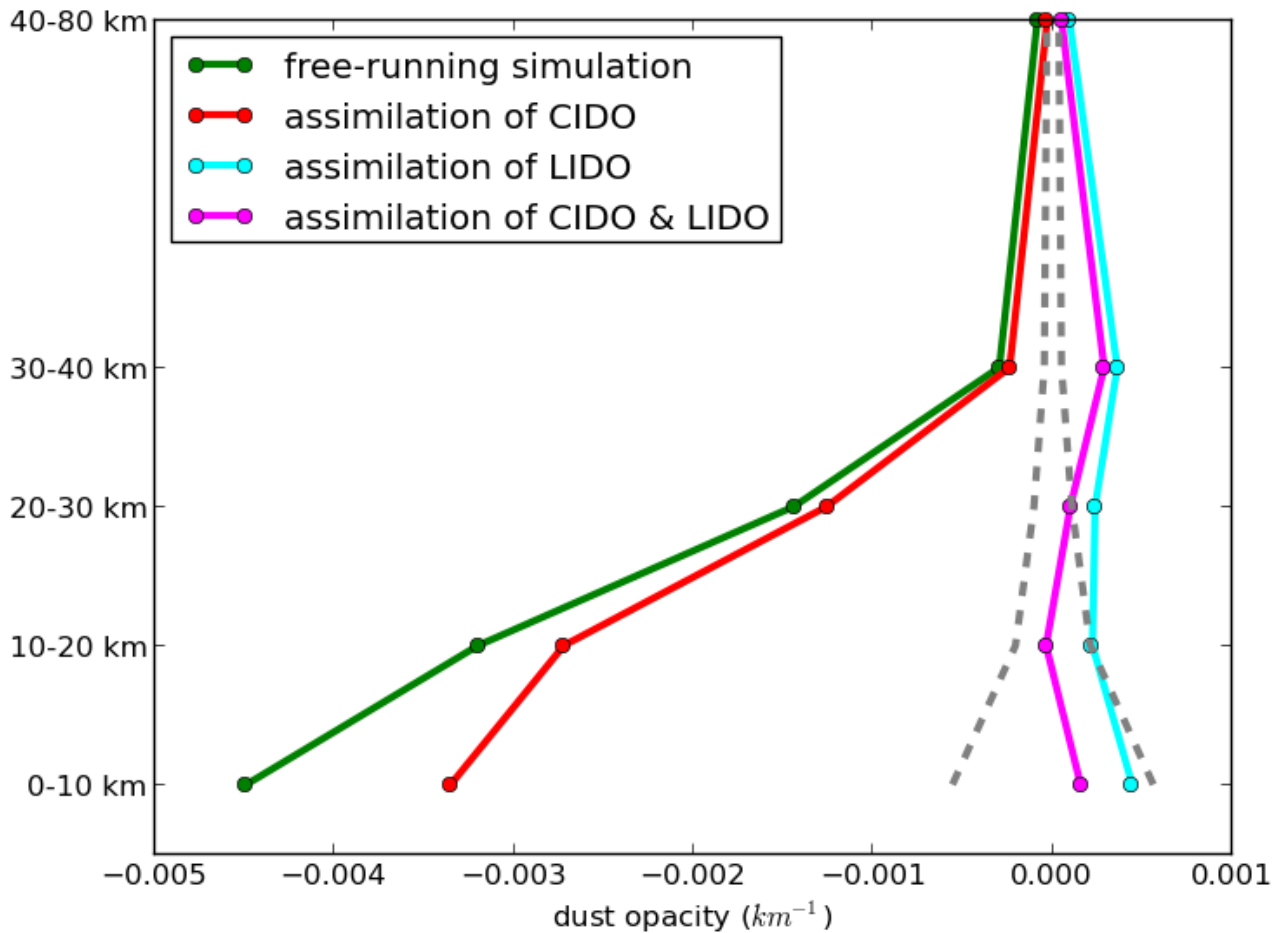


Figure S3. Global-time mean dust opacity difference between observed MCS dust opacities and the free-running model (green), CIDO-only reanalysis (red) LIDO-only reanalysis (cyan), and joint CIDO/LIDO reanalysis (magenta), during MY29 $L_s = 110^\circ - 330^\circ$. Grey dashed lines show the average error in the MCS observations.

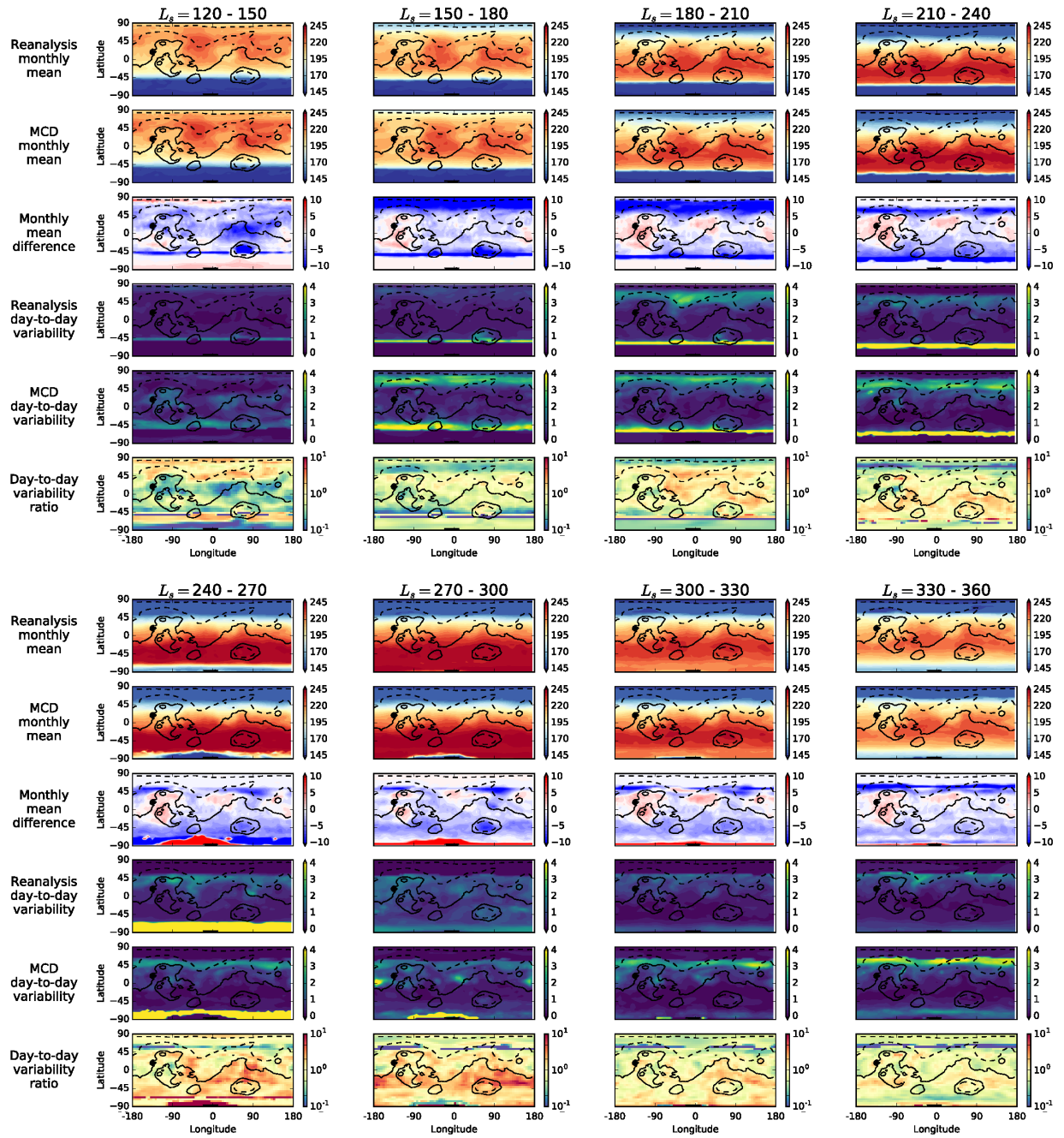


Figure S4. Surface temperature during MY28.

June 1, 2021, 3:49pm

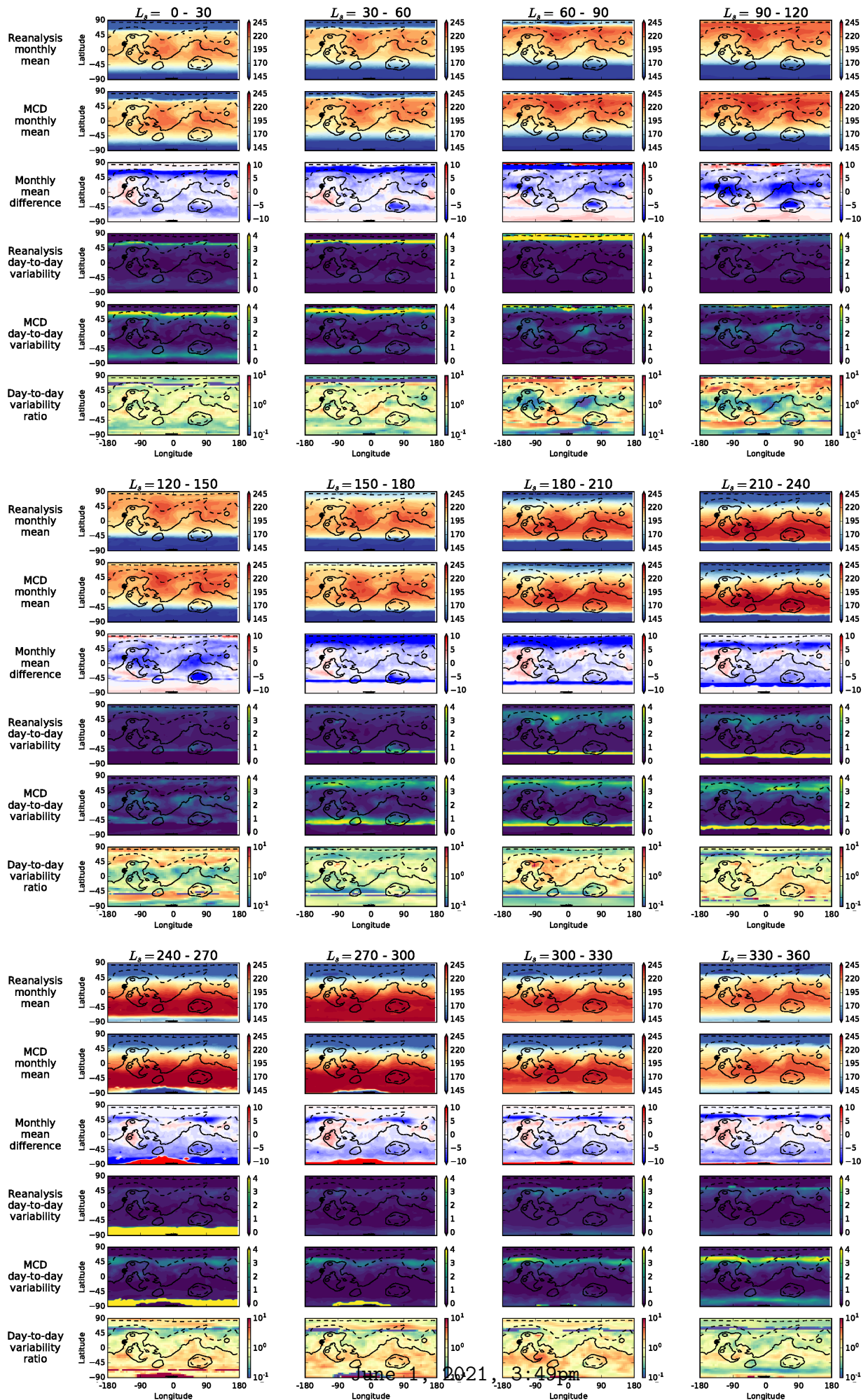


Figure S5. Surface temperature during MY29.

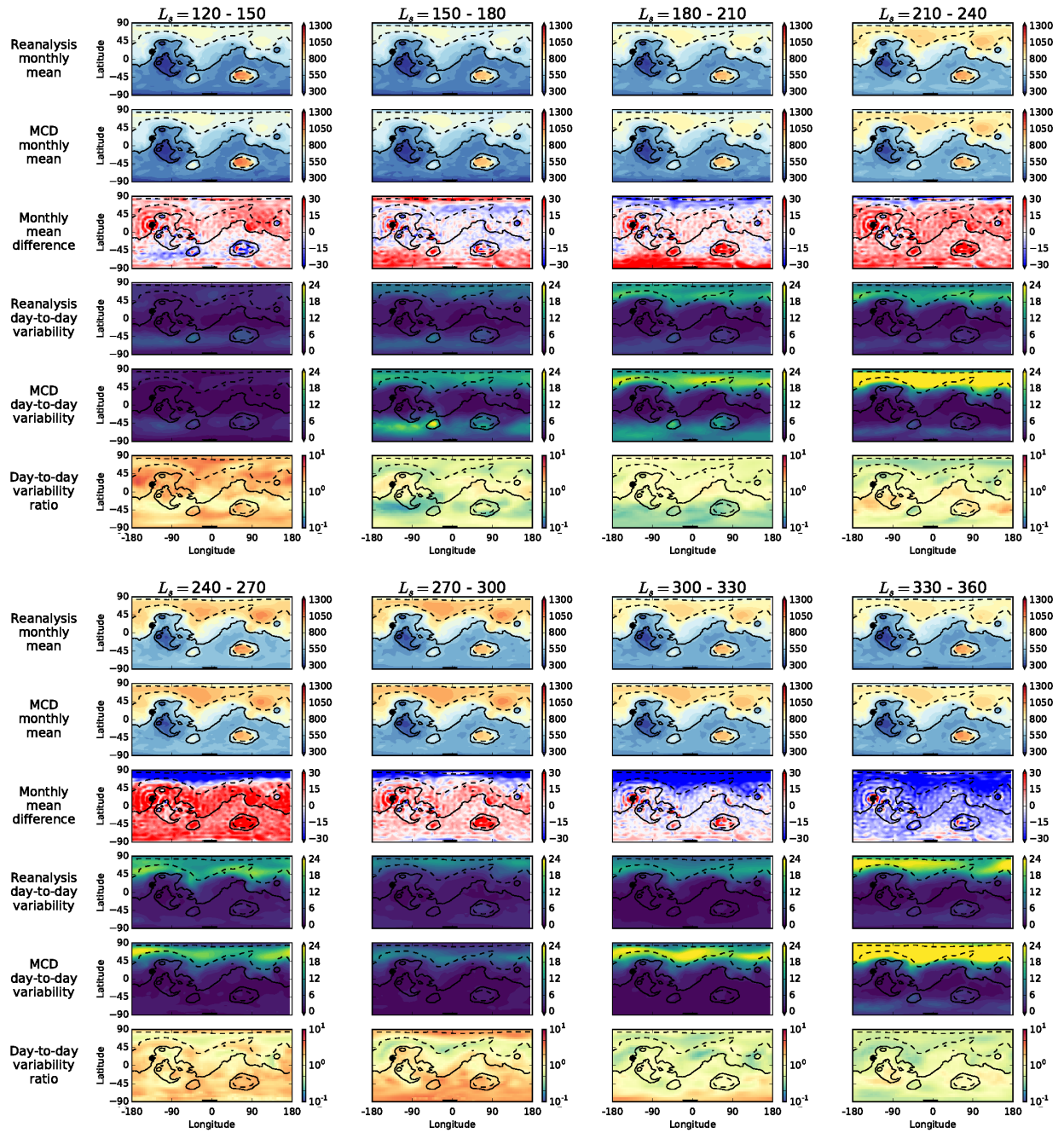


Figure S6. Surface pressure during MY28.

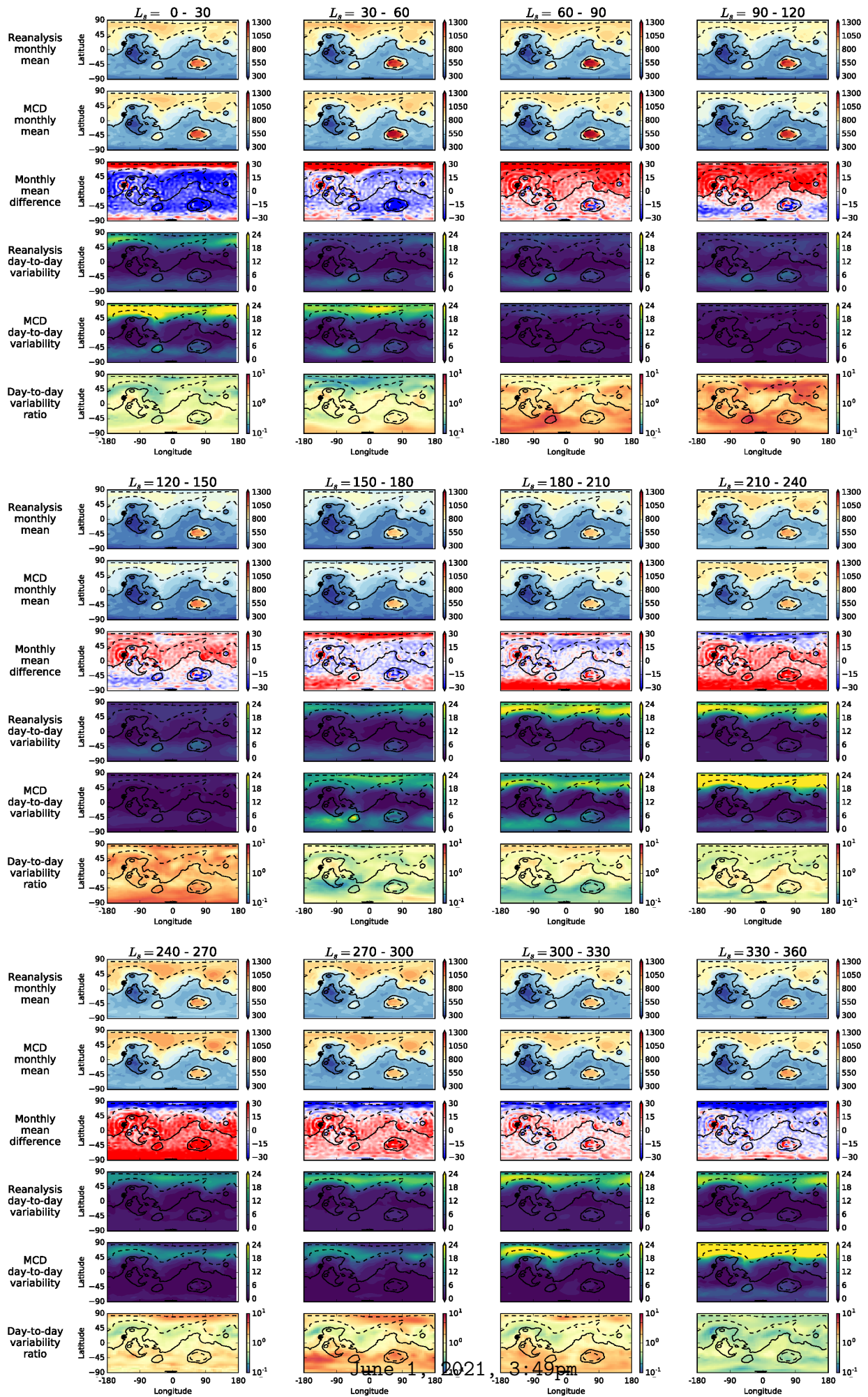


Figure S7. Surface pressure during MY29.

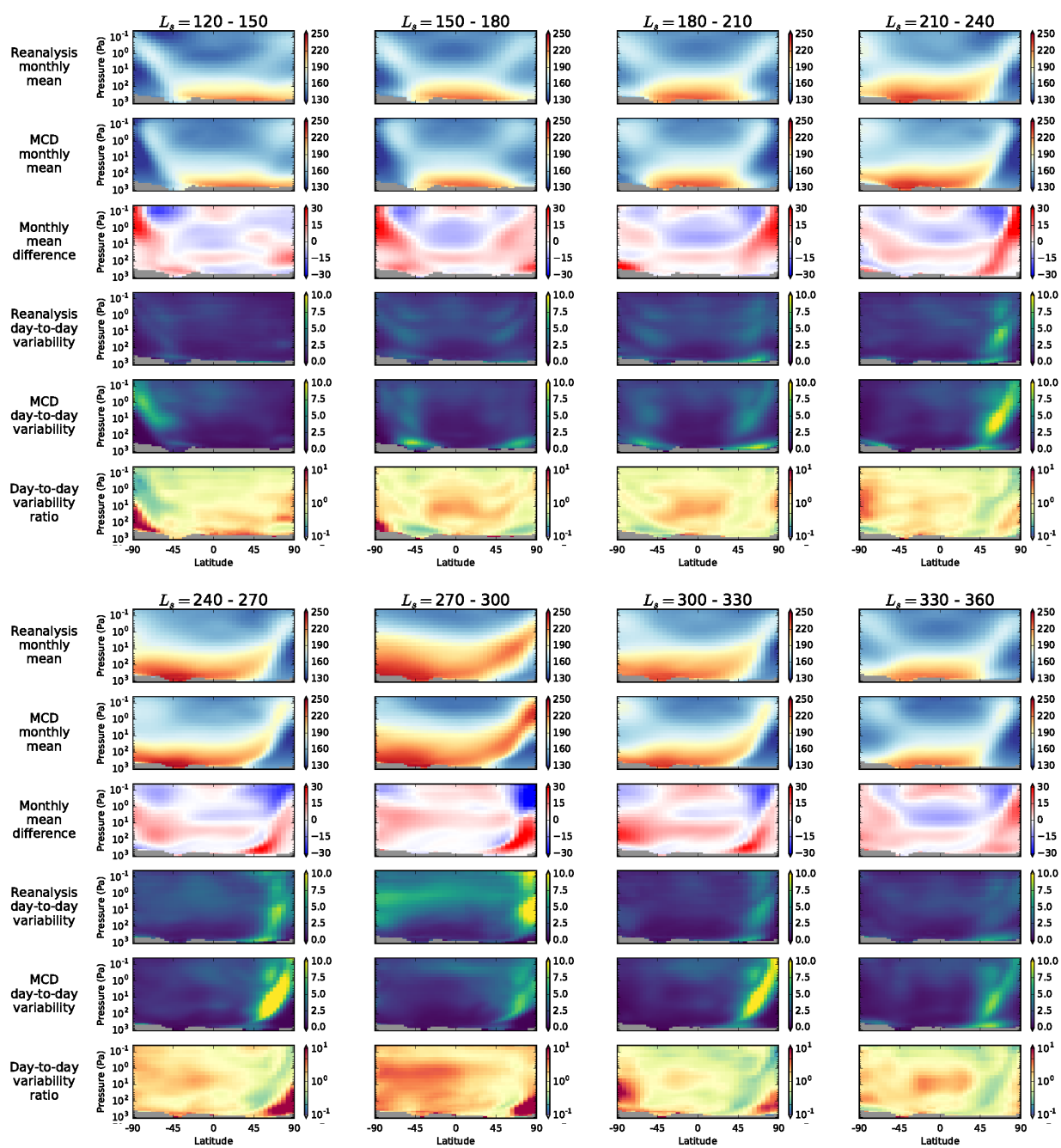


Figure S8. Zonal mean temperature during MY28.

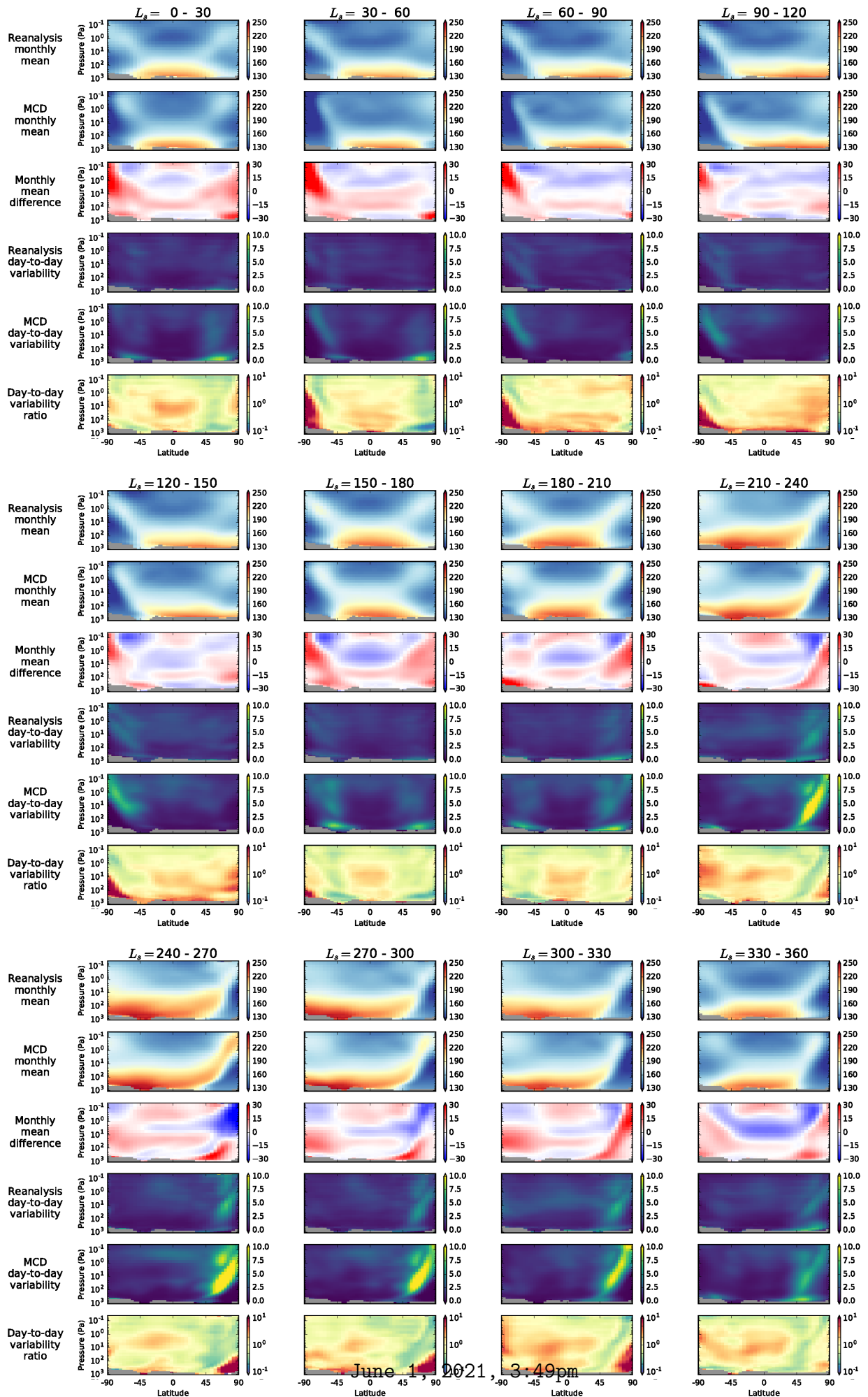


Figure S9. Zonal mean temperature during MY29.

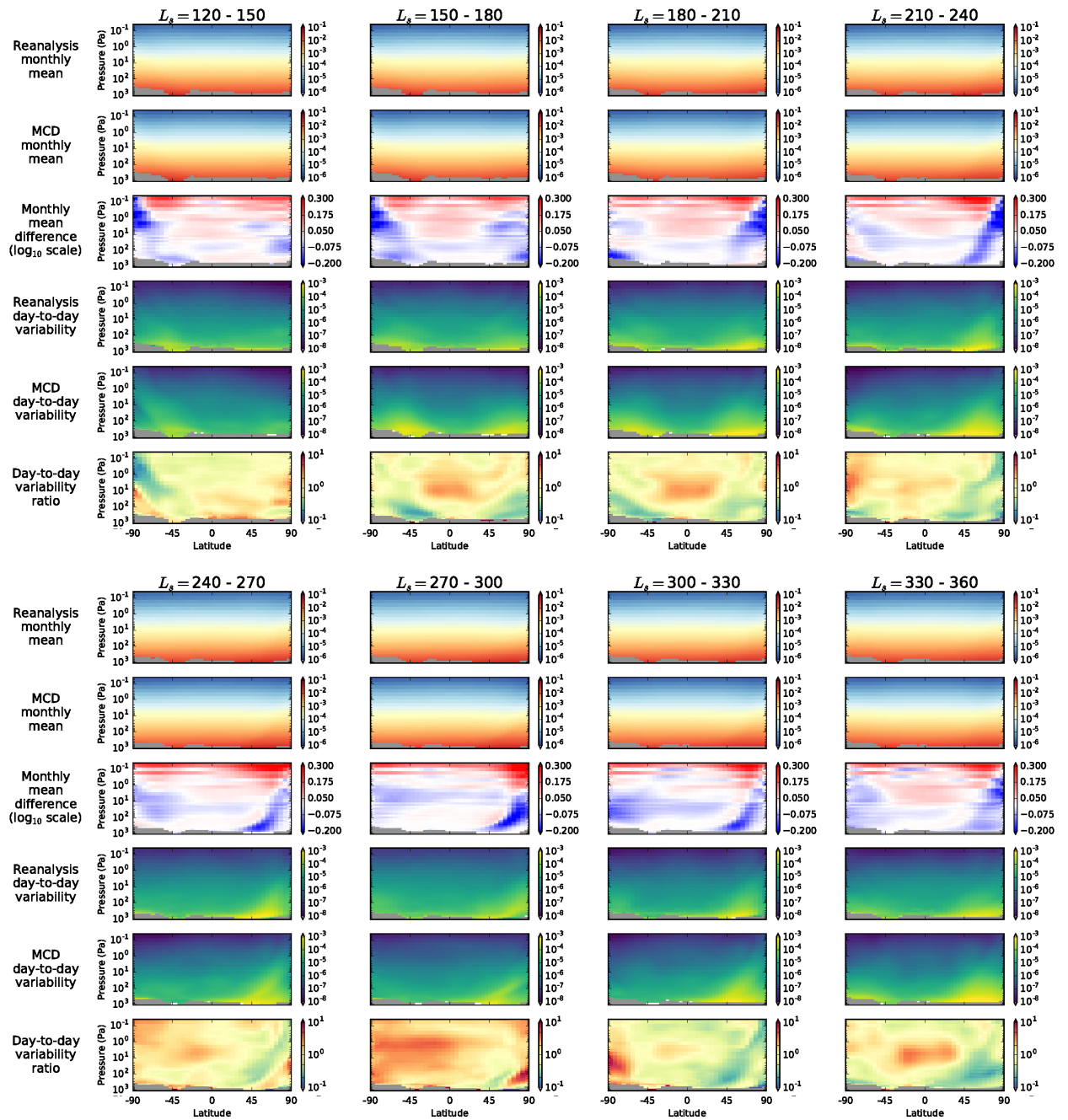


Figure S10. Zonal mean density during MY28.

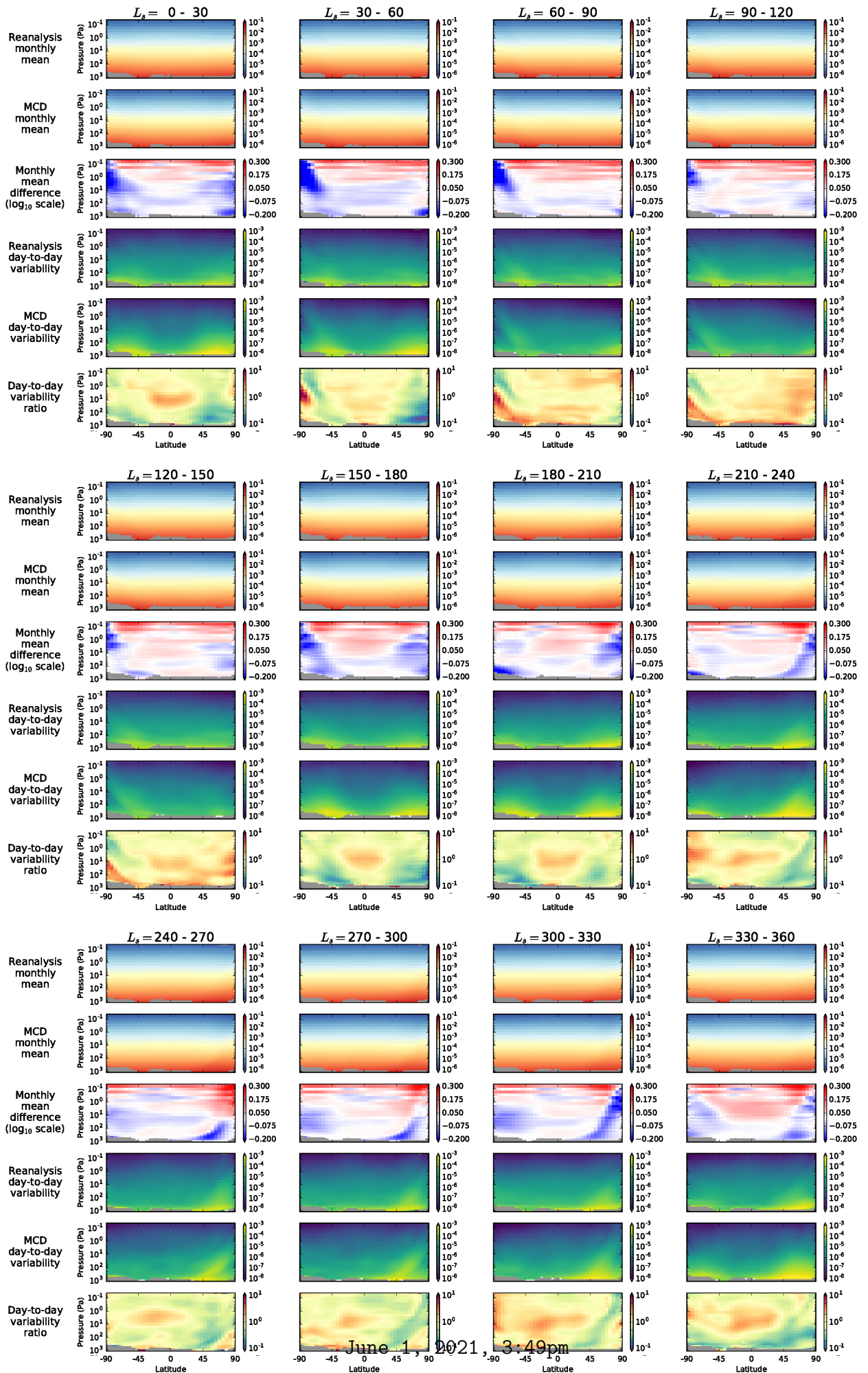


Figure S11. Zonal mean density during MY29.

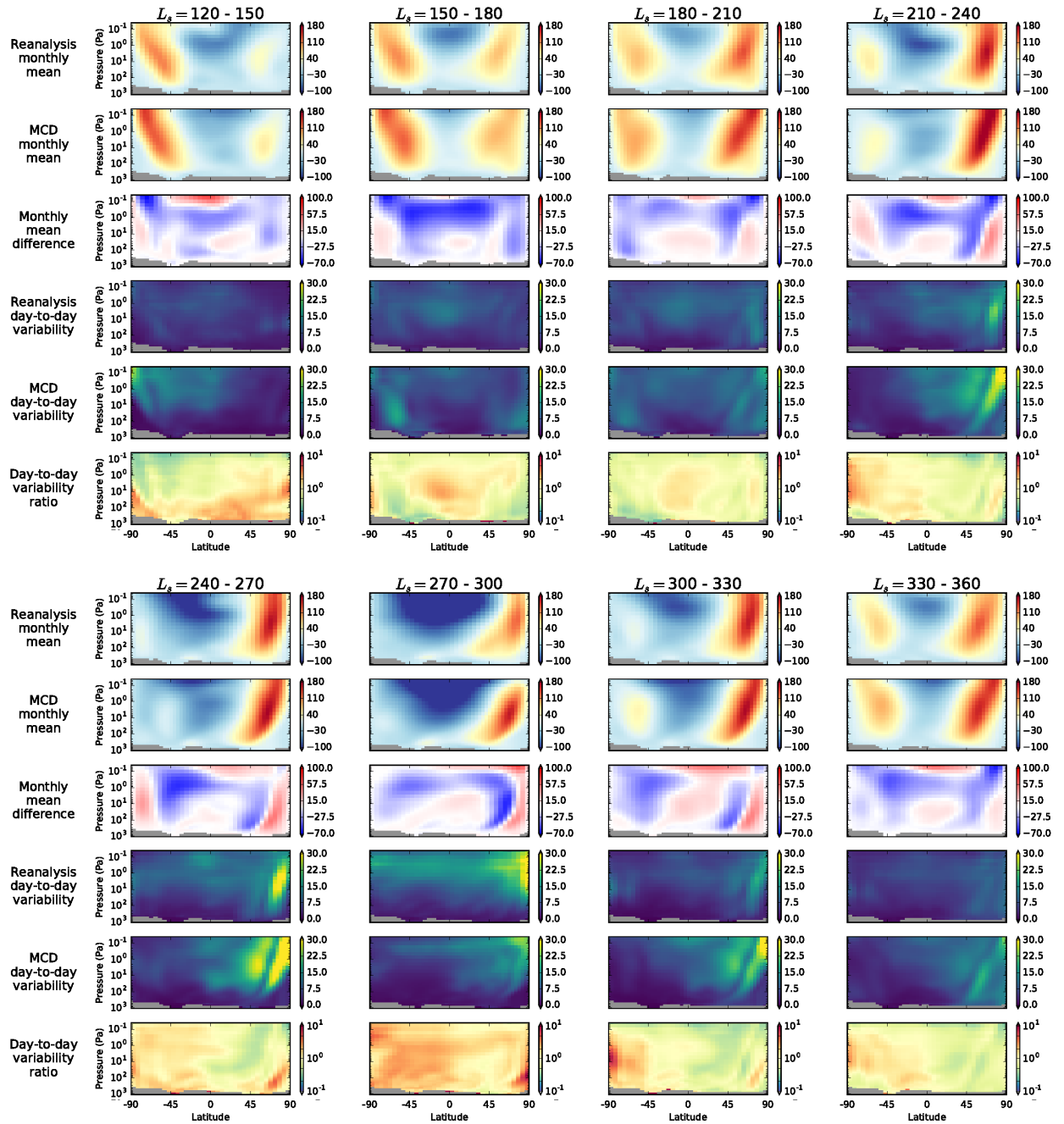


Figure S12. Zonal mean zonal velocity during MY28.

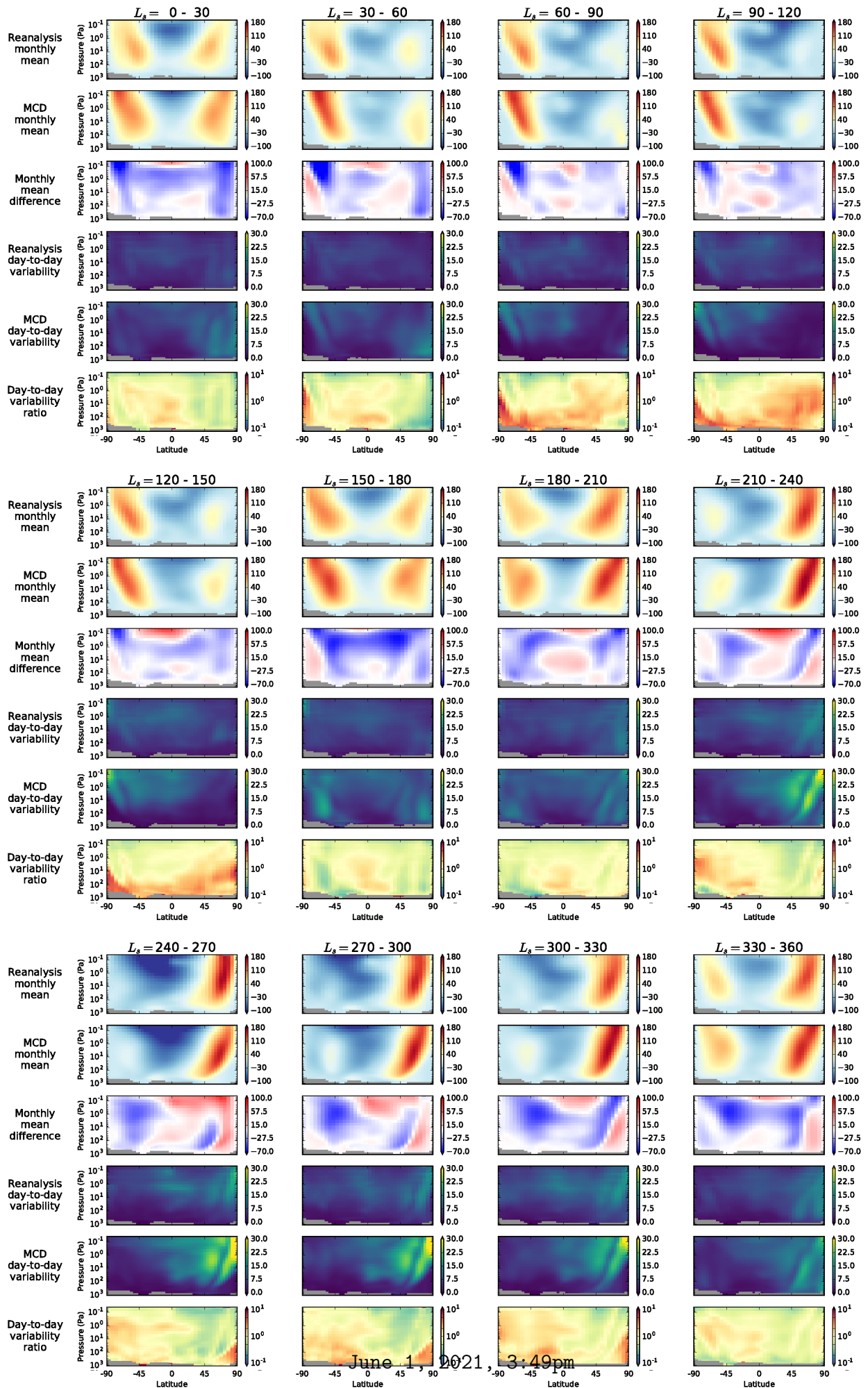


Figure S13. Zonal mean zonal velocity during MY29.

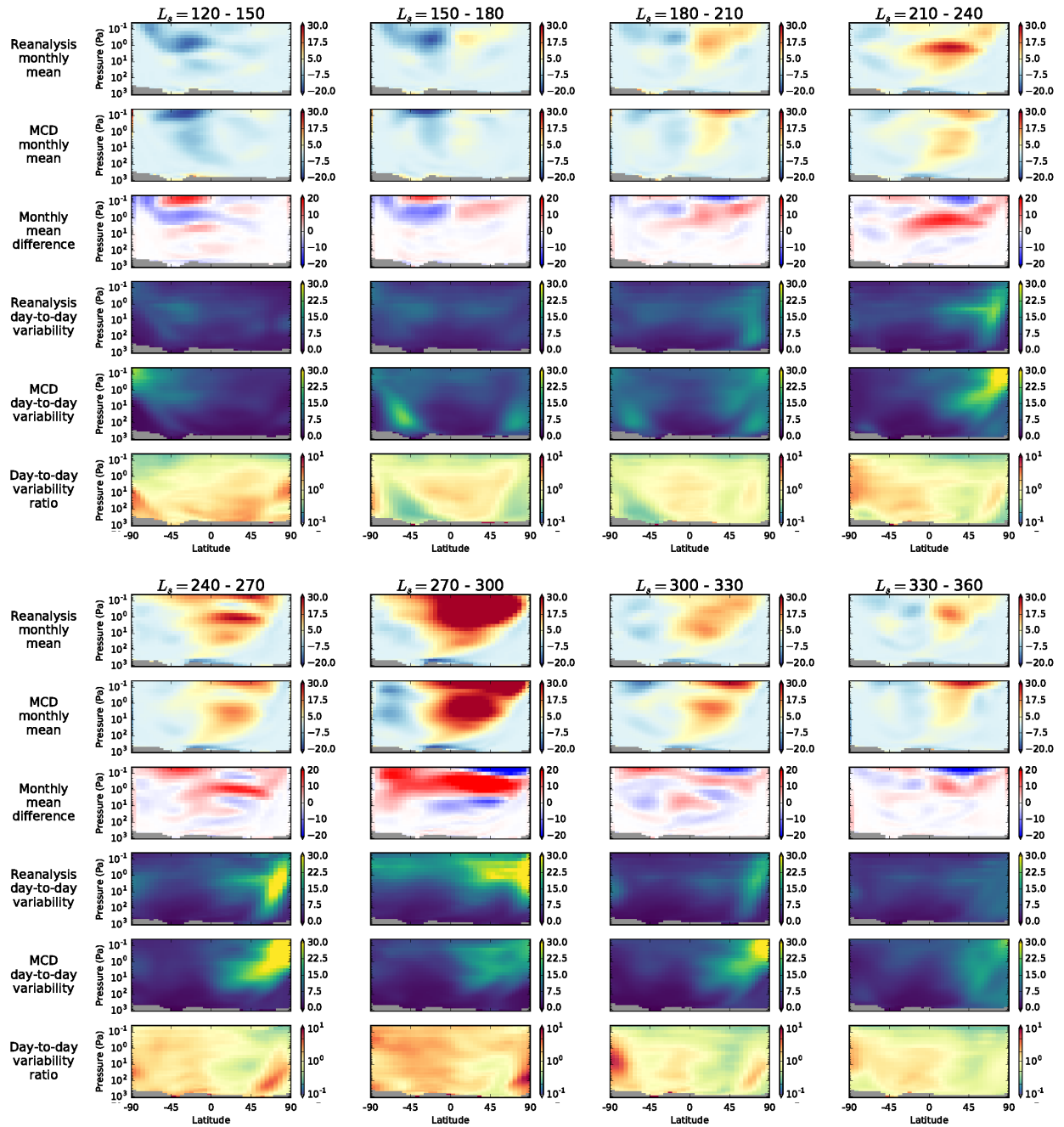


Figure S14. Zonal mean meridional velocity during MY28.

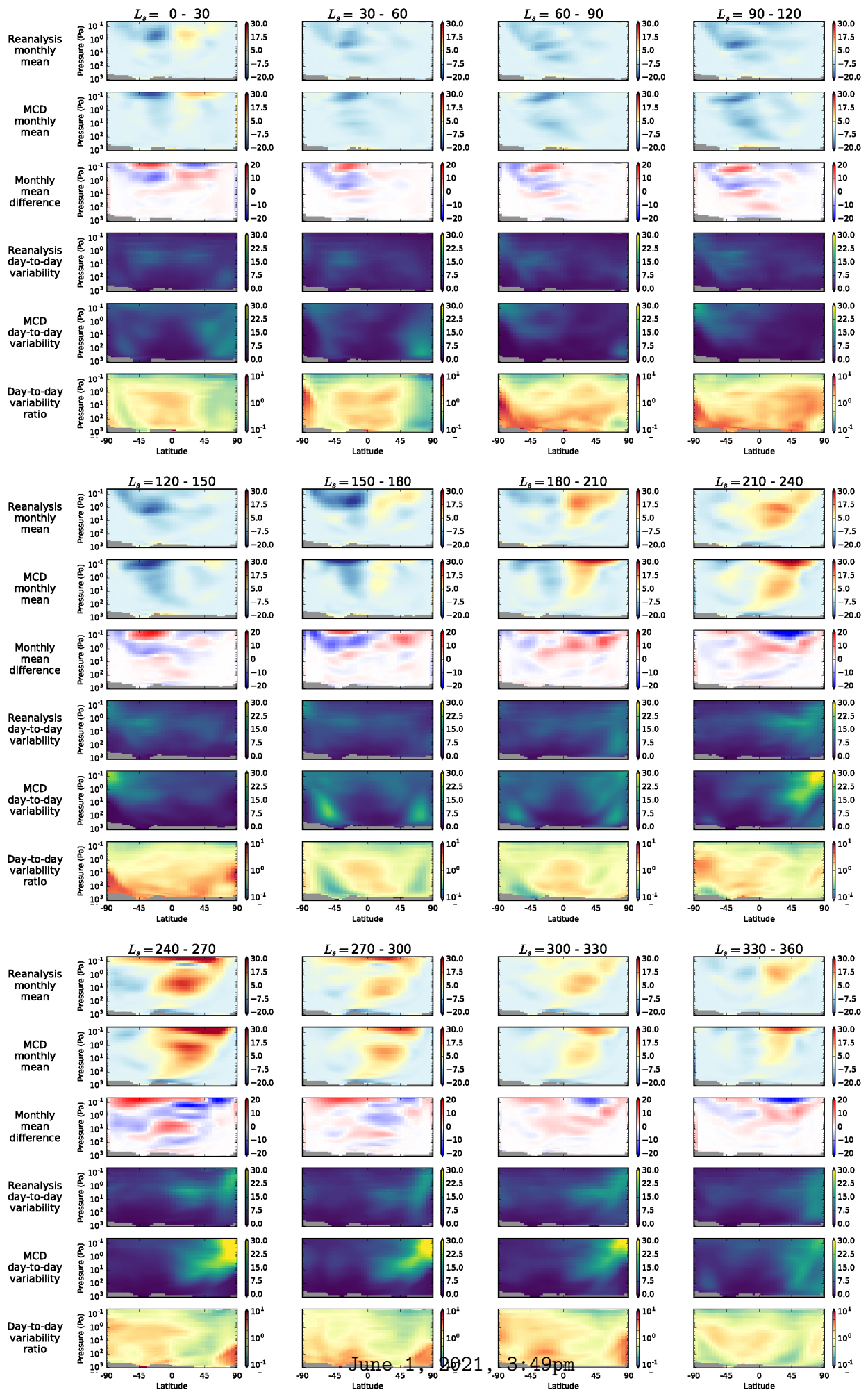


Figure S15. Zonal mean meridional velocity during MY29.